*T. Yagami*
*K. Kitagawa*
*C. Aida*
*H. Fujiwara*
*S. Futaki*

# Stabilization of a tyrosine *O*-sulfate residue by a cationic functional group: formation of a conjugate acid–base pair

**Authors' affiliations:**
*T. Yagami,* National Institute of Health Sciences, Tokyo, Japan.

*K. Kitagawa, C. Aida and H. Fujiwara,* Niigata College of Pharmacy, Niigata, Japan.

*S. Futaki,* Institute for Chemical Research, Kyoto University, Japan.

**Correspondence to:**
*Correspondence to: Dr Kouki Kitagawa*
*Niigata College of Pharmacy*
*5-13-2 Kamishin'ei-cho*
*Niigata*
*Niigata 950-2081*
*Japan*
*Tel.: 81-25-268-1241*
*Fax: 81-25-268-1230*
E-mail: kouki@niigata-pharm.ac.jp

**Dates:**
Received 17 December 1999;
Revised 7 March 2000;
Accepted 19 May 2000

**To cite this article:**
*Yagami, T., Kitagawa, K., Aida, C., Fujiwara, H. & Futaki, S.* Stabilization of a tyrosine *O*-sulfate residue by a cationic functional group: formation of a conjugate acid–base pair.
*J. Peptide Res.*, 2000, **56,** 239–249.



ISSN 1397–002X

**Key words:** cholecystokinin; conjugate acid–base pair; desulfation; gastrin II; liquid secondary-ion mass spectrometry; MALDI-TOFMS; sulfated tyrosine

**Abstract:** Sulfated tyrosine [Tyr($SO_3H$)]-containing peptides showed characteristic peak patterns in their liquid secondary-ion mass spectrometry (LSIMS) spectra. Protonated molecules were desulfated more easily than their deprotonated counterparts. Therefore, the stabilities of the Tyr($SO_3H$) residues were well-reflected by peak patterns in their positive-ion spectra. These intrinsic peak patterns were investigated by comparing the behavior of each Tyr($SO_3H$) residue in acidic solution. As the peptide chain was lengthened and the number of cationic functional groups increased, the peak representing the $[MH]^+$ of a Tyr($SO_3H$)-containing peptide became more prominent than that representing the desulfated $[MH–SO_3]^+$. These alterations in peptide structure also increased the stability of the Tyr($SO_3H$) residue in acidic solution. Based on the desulfation mechanism of an aryl monosulfate, we predicted that intramolecular cationic functional groups would stabilize Tyr($SO_3H$) residues by forming conjugate acid–base pairs (or salt bridges) both in the gaseous phase and in acidic solution. In accordance with this theory, Arg residues would take primary responsibility for this self-stabilization within Tyr($SO_3H$)-containing peptides. Moreover, a long peptide backbone was expected to have a weak protective effect against desulfation of the $[MH]^+$ in the gaseous phase. Tyr($SO_3H$) residues were also stabilized by adding an external basic peptide containing multiple Arg residues. Formation of such intermolecular acid–base pairs was demonstrated by matrix-assisted laser desorption/ionization time-of-flight mass spectrometry (MALDI-TOFMS) which detected conjugated peptide ions. The energetically favorable formation of conjugate acid–base pairs prompted by Tyr($SO_3H$) residues might be a driving force for protein folding and protein–protein interaction.

**Abbreviations:** AcOH, acetic acid; $AcONH_4$, ammonium acetate; Boc, *tert*-butyloxycarbonyl; CCK, cholecystokinin; DIPCDI, diisopropylcarbodiimide; DMF, *N*,*N*-dimethylformamide; Fmoc, fluoren-9-ylmethyloxycarbonyl; FT-IR, Fourier transform infrared spectrometry; G-II, gastrin-II; HOBt, 1-hydroxybenzotriazole; LSIMS, liquid secondary-ion mass spectrometry; MALDI-TOFMS, matrix-assisted laser desorption/ionization time-of-flight mass spectrometry; NMM, *N*-methylmorpholine; Pbf, 2,2,4,6,7-pentamethyldihydrobenzofuran-5-sulfonyl; RP-HPLC, reversed-phase high-performance liquid chromatography; *t*Bu, *tert*-butyl; TFA, trifluoroacetic acid

The sulfation of tyrosine residues is one of the ubiquitous post-translational modifications of peptides and proteins (1–3). This modification is catalyzed by tyrosylprotein sulfotransferase, a membrane-bound enzyme within the trans-Golgi compartment. It has been proposed that sulfate plays an important role in specific protein–protein interactions during protein transport. According to this theory, negative charges on tyrosine *O*-sulfate [Tyr($SO_3H$)] residues might participate in intermolecular recognition (3). They may also affect protein folding by interacting with cationic residues within Tyr($SO_3H$)-containing peptides. Despite its biological importance, this post-translational modification is hard to detect. It is well known that Tyr($SO_3H$) residues tend to rapidly desulfate to Tyr under acidic conditions. Thus, due to their intrinsic acid lability, traditional analytical methods, for example amino acid analysis of the acid hydrolysate or Edman degradation, cannnot be performed on peptides and proteins containing Tyr($SO_3H$) residues.

Since the late 1980s, mass spectrometry using soft-ionization techniques, such as fast atom bombardment ionization, MALDI and electrospray ionization, has seemed to be a very promising analytical tool for the examination of peptides and proteins containing Tyr($SO_3H$) residues (4–10). In previous studies, we observed characteristic fragmentation patterns in the positive- and negative-ion LSIMS spectra of peptides containing multiple Tyr($SO_3H$) residues (11). Moreover, we selectively detected the $[MH]^+$ of Tyr($SO_3H$)-containing peptides from crude peptide mixtures using constant neutral-loss (80 amu) scanning (12).

Both the appearance of characteristic fragmentation patterns and the ability to selectively detect Tyr($SO_3H$)-containing peptides could be explained by a proposed desulfation mechanism (13) (Fig. 1). According to this model, desulfation of aryl monosulfates, including Tyr($SO_3H$) residues, is catalyzed by protons and accelerated under nonpolar conditions. Indeed, it has been reported that

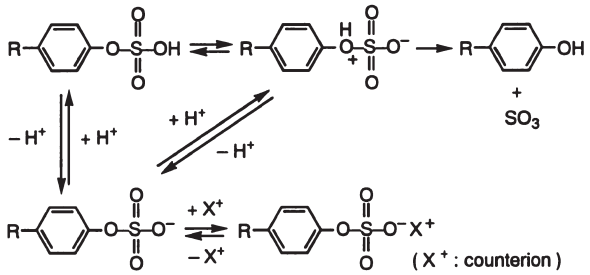


*Figure 1.* Plausible mechanism for desulfation and stabilization of a Tyr($SO_3H$) residue.

Tyr($SO_3H$) residues rapidly decompose to Tyr residues in nonpolar organic solvents, as well as in strongly acidic solutions (14,15). Accordingly, we can rationally predict that the proton-surplus $[MH]^+$ of Tyr($SO_3H$)-containing peptides rapidly loses its sulfate in the gaseous phase (a nonpolar environment). As a result, the completely desulfated fragment ion, $[MH–nSO_3]^+$, where $n$ represents the number of Tyr($SO_3H$) residues, should appear prominently in the positive-ion spectrum. The remarkable lability of the $[MH]^+$ also allows its selective detection by constant neutral-loss (80 amu) scanning. In contrast to $[MH]^+$, the proton-deficient $[M–H]^-$ of Tyr($SO_3H$)-containing peptides must be relatively stable even in the gaseous phase. We expect that at least one Tyr($SO_3H$) residue should remain intact without becoming an amphoteric ion subject to desulfation. As a result, the characteristic ladder fragmentation pattern, $[M–H–mSO_3]^-$ ($m$=1,2,..., $n$–1), should appear in the negative-ion spectrum.

From the same desulfation mechanism (Fig. 1), we predicted that Tyr($SO_3H$) residues become stable by forming conjugate acid–base pairs or ion pairs with cations other than protons. Intramolecular cationic functional groups are candidates for the conjugate base. If such conjugate acid–base pairs are actually formed, Tyr($SO_3H$) residues would become stable not only in acidic solutions, but also in the gaseous phase. In order to investigate this assumption, we first compared the stability of Tyr($SO_3H$) residues within various sulfated peptides in the gaseous phase and in acidic solution.

## Experimental Procedures

Fluoren-9-ylmethyloxycarbonyl (Fmoc) amino acid derivatives and 2-chlorotrityl (Clt) resin (16) (substituted level; 1.47 mmol/g) were purchased from Watanabe Chemical Co., Ltd. (Hiroshima, Japan). Other chemicals were of analytical grade. Authentic samples of tyrosine-*O*-sulfated Leu-enkephalin [H-Tyr($SO_3H$)-Gly-Gly-Phe-Leu-OH] (17) and CCK-8

were obtained from the Peptide Institute, Inc. (Osaka, Japan). Peptides used in the MALDI-TOFMS study [H-RRLSSLRA-OH (S6-1), Ac-MLF-OH and H-KHG-$NH_2$ (Bursin)] were purchased from Novabiochem (Tokyo, Japan). The amino acid composition of an acid hydrolysate was determined using a Hitachi 8500 model amino acid analyzer. FT-IR spectra were recorded on a Perkin–Elmer 1720 spectrometer. RP-HPLC was performed on a Hitachi L-6200 model.

### Synthesis of sulfated peptides

#### CCK peptides and G-II peptides

Human cholecystokinin (CCK) and gastrin-II (G-II) peptides (Table 1) were prepared using the facile solid-phase method developed by Kitagawa *et al*. (18). The purity of each peptide exceeded 98% on RP-HPLC. Details of their syntheses are reported elsewhere.

#### *N*-Acetyl tyrosine-*O*-sulfated Leu-enkephalin

*N*-Acetyl tyrosine-*O*-sulfated Leu-enkephalin was prepared using Fmoc-Leu-Clt-resin (0.15 mmol) as a starting material. Each residue including Fmoc-Tyr($SO_3Na$)-OH (19,20) was introduced using the DIPCDI/HOBt coupling protocol [Fmoc-amino acid (3 eq.), DIPCDI (3 eq.) and HOBt (3 eq.); 90 min]. After introducing the N-terminal Tyr($SO_3Na$) residue, the free α-amino group was acetylated with acetic anhydride (1.0 mmol) in the presence of pyridine (1.0 mmol). The peptide-resin obtained (50 mg) was treated with a mixture of AcOH/trifluoroethanol/$CH_2Cl_2$ (1 : 1 : 3 v/v, 5 mL) for 20 min at 20°C, then filtered. After the filtrate had been concentrated with a stream of $N_2$, dry ether (50 mL) was added to it. The resultant precipitate was collected by centrifugation and lyophilized from 0.025 M $NH_4HCO_3$ (30 mL); weight 9.80 mg. Part of the crude peptide was purified by RP-HPLC [HPLC conditions: column, Cosmosil 5$C_{18}$-AR (10×250 mm); elution system, a linear gradient of $CH_3CN$/0.1 M $AcONH_4$ (20–25% in 60 min); flow rate, 2.5 mL/min; absorbance was detected at 265 nm]. The integrity of the sulfate was confirmed by FT-IR (1050 $cm^{-1}$).

#### CCK-12 derivatives

[Lys$^4$], [Leu$^4$] and [Glu$^4$]CCK-12, [H-Ile-Ser-Asp-**X**-Asp-Tyr($SO_3H$)-Met-Gly-Trp-Met-Asp-Phe-$NH_2$; **X**=Lys, Leu, or Glu], were prepared from 0.1 mmol of Fmoc-Asp (Clt resin)-Phe-$NH_2$ (18,21) (Fig. 2). The DIPCDI/HOBt coupling protocol was used to elongate each derivative. After assembly, the protected peptide-resin (≈ 80 mg) was treated with a mixture of AcOH/trifluoroethanol/$CH_2Cl_2$ (1 : 1 : 3, 4 mL) at 25°C for 20 min; the detached peptide was then treated with 90% aqueous TFA (2 mL) at 0°C for 7 h. The crude peptide was purified by RP-HPLC [column, μBondasphere 5$C_{18}$ 100 Å (19×150 mm); elution system, a linear gradient of $CH_3CN$/0.1 M $AcONH_4$ at a flow rate of 1.75 mL/min; absorbance was detected at 265 nm]. Yields of the purified peptides were between 31 and 37% based on the protected peptide-resin. Amino acid ratios of the acid hydrolyzates were as follows: [Lys$^4$]CCK-12, Asp 3.03, Ser 0.90, Gly 1.00, Met 1.74, Ile 1.05, Tyr 1.00, Phe 0.96, Lys 1.04, Trp ND (not determined); [Leu$^4$]CCK-12, Asp 2.96, Ser 0.88, Gly 1.00, Met 1.43, Ile 1.01, Leu 1.00, Tyr 0.98, Phe 0.95, Trp ND; [Glu$^4$]CCK-12, Asp 3.03, Ser 0.89, Glu 1.03, Gly 1.00, Met 1.53, Ile 1.04, Tyr 1.01, Phe 0.96, Trp ND. The integrity of the sulfate was confirmed by FT-IR (1049 $cm^{-1}$). The detected molecular mass (monoisotopic mass) of each peptide coincided with calculated values.

#### Cionin

The protochordate-derived cionin [H-Asn-Tyr($SO_3H$)-Tyr($SO_3H$)-Gly-Trp-Met-Asp-Phe-$NH_2$] was prepared using the Fmoc-based solid-phase approach (22).

***Table 1.*** **Amino acid sequences of CCK and G-II peptides**

| | |
|---|---|
| CCK Peptides | |
| CCK-8 | H-Asp-*Tyr($SO_3H$)*-Met-Gly-Trp-Met-Asp-Phe-$NH_2$ |
| CCK-12 | H-Ile-Ser-Asp-Arg-Asp-*Tyr($SO_3H$)*-Met-Gly-Trp-Met-Asp-Phe-$NH_2$ |
| CCK-22 | H-Asn-Leu-Gln-Asn-Leu-Asp-Pro-Ser-His-Arg-Ile-Ser-Asp-Arg-Asp-*Tyr($SO_3H$)*-Met-Gly-Trp-Met-Asp-Phe-$NH_2$ |
| CCK-33 | H-Lys-Ala-Pro-Ser-Gly-Arg-Met-Ser-Ile-Val-Lys-Asn-Leu-Gln-Asn-Leu-Asp-Pro-Ser-His-Arg-Ile-Ser-Asp-Arg-Asp-*Tyr($SO_3H$)*-Met-Gly-Trp-Met-Asp-Phe-$NH_2$ |
| G-II Peptides | |
| mini gastrin-II (G-14) | H-Trp-Leu-Glu-Glu-Glu-Glu-Glu-Ala-*Tyr($SO_3H$)*-Gly-Trp-Met-Asp-Phe-$NH_2$ |
| little gastrin-II (G-17) | Pyr-Gly-Pro-Trp-Leu-Glu-Glu-Glu-Glu-Glu-Ala-*Tyr($SO_3H$)*-Gly-Trp-Met-Asp-Phe-$NH_2$ |
| big gastrin-II (G-34) | Pyr-Leu-Gly-Pro-Gln-Gly-Pro-Pro-His-Leu-Val-Ala-Asp-Pro-Ser-Lys-Lys-Gln-Gly-Pro-Trp-Leu-Glu-Glu-Glu-Glu-Glu-Ala-*Tyr($SO_3H$)*-Gly-Trp-Met-Asp-Phe-$NH_2$ |

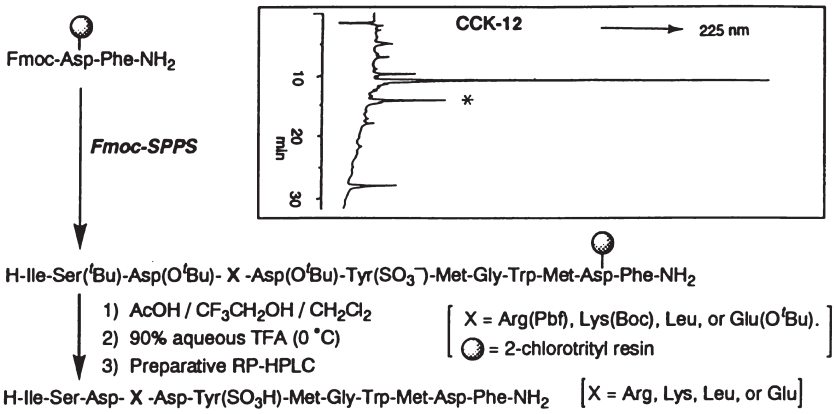


*Figure 2.* Synthetic scheme for CCK-12 and its derivatives. Inset: RP-HPLC chromatogram of crude CCK-12 (**X**=Arg) obtained after deprotection. An asterisk shows the peak representing the desulfated peptide (CCK-12 nonsulfate). HPLC conditions [column, Cosmosil $5C_{18}$ AR (4.6×150 mm); elution system, a linear gradient of $CH_3CN$/0.1 M $AcONH_4$ (20–35% in 30 min); flow rate, 1 mL/min; absorbance was detected at 225 nm].

### Desulfation rates of Tyr($SO_3H$)-containing peptides in acidic solution

HPLC-purified G-17 (540 µg) was dissolved in an ice-cooled mixture of $CH_3CN$ and $H_2O$ (2 : 3 v/v, 500 µL) containing 5% TFA, and then incubated at 37°C. An aliquot of the solution was withdrawn at appropriate intervals (0.5, 1, 2, 3 and 5 h) and immediately lyophilized. Each lyophilizate was reconstituted with ice-cooled 15% $CH_3CN$ in 0.1 M $AcONH_4$ (100 µL), 20 µL of this solution was then applied to RP-HPLC [column, Cosmosil $5C_{18}$-AR (3.9×150 mm); elution system, a linear gradient of $CH_3CN$/0.1 M $AcONH_4$ (17–32% in 30 min); flow rate,1 mL/min; absorbance was detected at 225 nm].

Desulfation of the other peptides was similarly examined. Retention times of intact peptides and their nonsulfated counterparts are listed in Table 2, along with the molecular masses of the sulfated forms.

### Mass spectrometry

LSIMS spectra were obtained using a VG ZAB-2SE double-focusing mass spectrometer (VG Analytical, Ltd, Manchester, UK) with an OPUS operating data system. Each HPLC-purified peptide was dissolved in a mixture of $H_2O/CH_3CN$ (1 : 1) at a concentration of ≈ 10 µg/µL. Glycerol, thioglycerol and *m*-nitrobenzyl alcohol were used as the matrix, either neat or in combination. Typically, 2 µL of matrix was deposited on the target, and 1 µL of the peptide solution was added and mixed with the matrix. Ionization of the sample was performed using ≈ 1 µA of cesium ions which were applied with a cesium ion gun. All spectra were recorded at

***Table 2.*** **Molecular masses and retention times of CCK and G-II peptides**

| | | | $t_R$ on HPLC (min)[a] | |
|---|---|---|---|---|
| Temp | Formula and molecular mass | | Sulfate | Nonsulfate |
| CCK Peptides | | | 20–35% in 30 min | |
| CCK-8 | $C_{49}H_{62}N_{10}O_{16}S_3$ | 1142.4[b] | 13.4 | 16.4 |
| CCK-12 | $C_{68}H_{95}N_{17}O_{23}S_3$ | 1613.6[b] | 12.0 | 15.4 |
| CCK-22 | $C_{117}H_{173}N_{35}O_{39}S_3$ | 2790.0[c] | 15.1 | 17.3 |
| CCK-33 | $C_{167}H_{263}N_{51}O_{52}S_4$ | 3945.5[c] | 24.7[d] | 26.5[d] |
| [$Lys^4$]CCK-12 | $C_{68}H_{95}N_{15}O_{23}S_3$ | 1585.6[b] | 8.7 | 12.4 |
| [$Leu^4$]CCK-12 | $C_{68}H_{94}N_{14}O_{23}S_3$ | 1570.6[b] | 11.8 | 16.2 |
| [$Glu^4$]CCK-12 | $C_{67}H_{90}N_{14}O_{25}S_3$ | 1586.5[b] | 5.5 | 9.8 |
| G-II Peptides | | | 17–32% in 30 min | |
| G-14 | $C_{85}H_{109}N_{17}O_{30}S_2$ | 1913.0[c] | 14.3 | 18.0 |
| G-17 | $C_{97}H_{123}N_{20}O_{34}S_2$ | 2177.3[c] | 15.0 | 17.9 |
| G-34 | $C_{176}H_{251}N_{43}O_{56}S_2$ | 3929.3[c] | 17.7 | 19.5 |

a. HPLC conditions: column, Cosmosil $5C_{18}$ AR (4.6×150 mm); elution system, a linear gradient of $CH_3CN$/0.1 M $AcONH_4$; flow rate,1 mL/min; absorbance was detected at 225 nm. b. Calculated as monoisotopic mass. c. Calculated as average mass. d. 20–40% in 60 min at a flow rate of 1 mL/min.

an accelerating voltage of 8 kV and at a resolution of 1000. The scan rate was chosen so that each scan took ≈ 20 s, and data from several scans were generally summed over the course of 1–2 min. Data accumulated in multichannnel analyzer (MCA) mode were processed by standard practices employed by the software. No corrections were made to account for background from the matrix. Mass calibration was carried out using clusters of cesium iodide to set an external standard. The pseudo-molecular ions of peptides that exceed a molecular mass of 1700 Da, are shown as average masses (Table 2).

In order to examine the possibility that desulfation could occur in the matrix during mass spectrometric analysis, CCK-8 was dissolved in glycerol and measured. After being bombarded for 3 min with cesium ions, the sample was withdrawn from the target and examined by RP-HPLC [column, Wakosil-II $5C_{18}$ (4.6×150 mm); elution system, a linear gradient of $CH_3CN$/0.1 M $AcONH_4$ (15–45% in 30 min); flow rate, 1 mL/min; absorbance was detected at 280 nm].

#### MALDI-TOFMS

MALDI-TOFMS spectra were obtained using a Shimadzu/Kratos Kompact MALDI IV time-of-flight mass spectrometer fitted with a nitrogen laser (337 nm). Either CCK-8 or cionin was dissolved in $H_2O/CH_3CN$ (1 : 1, v/v) and mixed with 5 eq. of a peptide (S6-1, Ac-MLF-OH or H-KHG-$NH_2$). The mass spectrum of each mixture was recorded in linear mode at a 20-kV accelerating voltage using sinapinic acid as the matrix for ionization. Pseudo-molecular ions registered on MALDI-TOFMS spectra as average masses.

## Results

#### LSIMS spectra of CCK peptides

The positive- and negative-ion LSIMS spectra of CCK peptides are shown in Fig. 3. In the positive-ion spectrum of CCK-8 (the shortest CCK peptide examined), a prominent $[MH–SO_3]^+$ peak (*m/z* 1063.3) accompanied a weak $[MH]^+$ peak (*m/z* 1143.3). However, there were significant changes within the peak patterns in the positive-ion spectra of CCK peptides as peptide lengths were altered. In the spectrum of CCK-12, the $[MH]^+$ (*m/z* 1614.5) and the $[MH–SO_3]^+$ (*m/z* 1534.6) were detected at an almost equal intensity. However, in the spectra of CCK-22 and CCK-33, the peak representing the $[MH]^+$ of each peptide (*m/z* 2791.1 for CCK-22 and 3946.5 for CCK-33) became more prominent than that of the desulfated $[MH–SO_3]^+$ which exhibited negligible intensity. These peak patterns were not significantly affected by changing the matrix for ionization. In contrast, the peak representing the $[M–H]^-$ of each peptide (*m/z* 1141.3 for CCK-8, 1612.5 for CCK-12, 2788.9 for CCK-22 and 3944.6 for CCK-33) appeared consistently as the base peak in the negative-ion LSIMS spectra. We could not detect any desulfated CCK-8 on a RP-HPLC chromatogram even after CCK-8 was exposed to a 3-min measurement of its LSIMS spectrum in the positive-ion mode.

#### LSIMS spectra of G-II peptides

The positive- and negative-ion LSIMS spectra of G-II peptides are shown in Fig. 4. In the positive-ion spectra of G-14 and G-17, the base peaks were the desulfated $[MH–SO_3]^+$ (*m/z* 1833.7 for G-14 and 2098.4 for G-17). The peaks corresponding to the $[MH]^+$ (*m/z* 1913.8 for G-14 and 2178.1 for G-17) were very weak. In the positive-ion spectrum of G-34, a prominent $[MH]^+$ peak (*m/z* 3929.9) accompanied a weak $[MH–SO_3]^+$ peak (*m/z* 3849.0). The $[M–H]^-$ peak of each peptide (*m/z* 1911.9 for G-14, 2176.3 for G-17, and 3927.8 for G-34) appeared consistently as the base peak in the negative-ion LSIMS spectra.

#### Stability of the Tyr($SO_3H$) residues in acidic solution

In general, short peptides tended to desulfate more easily than longer ones in acidic solution (Fig. 5). This tendency was especially pronounced in CCK peptides; the order of the desulfation rate was CCK-8>CCK-12>CCK-22>CCK-33. However, size dependency could not be substantiated in G-II peptides; G-17 was most susceptible to desulfation and G-14 was exceptionally stable in acidic solution.

#### Effects of cationic functional groups in Tyr($SO_3H$)-containing peptides on the positive-ion LSIMS spectra and desulfation rates

First, the positive-ion LSIMS spectra of tyrosine-*O*-sulfated Leu-enkephalin and its *N*-acetylated derivative were compared. In the spectrum of sulfated Leu-enkephalin, the $[MH]^+$ peak (*m/z* 636.2) and the desulfated $[MH–SO_3]^+$ peak (*m/z* 556.3) were detected at comparable intensities. In contrast, a prominent $[MH–SO_3]^+$ peak (*m/z* 598.3) and a weak $[MH]^+$ peak (*m/z* 678.3) were detected in the spectrum of the *N*-acetylated derivative. The relative dominance of $[MH]^+$ over $[MH–SO_3]^+$ was well correlated with the stability

DOCKET ALARM

# Explore Litigation Insights

Docket Alarm provides insights to develop a more informed litigation strategy and the peace of mind of knowing you're on top of things.

## Real-Time Litigation Alerts

Keep your litigation team up-to-date with **real-time alerts** and advanced team management tools built for the enterprise, all while greatly reducing PACER spend.

Our comprehensive service means we can handle Federal, State, and Administrative courts across the country.

## Advanced Docket Research

With over 230 million records, Docket Alarm's cloud-native docket research platform finds what other services can't. Coverage includes Federal, State, plus PTAB, TTAB, ITC and NLRB decisions, all in one place.

Identify arguments that have been successful in the past with full text, pinpoint searching. Link to case law cited within any court document via Fastcase.

## Analytics At Your Fingertips

Learn what happened the last time a particular judge, opposing counsel or company faced cases similar to yours.

Advanced out-of-the-box PTAB and TTAB analytics are always at your fingertips.

## API

Docket Alarm offers a powerful API (application programming interface) to developers that want to integrate case filings into their apps.

**LAW FIRMS**
Build custom dashboards for your attorneys and clients with live data direct from the court.

Automate many repetitive legal tasks like conflict checks, document management, and marketing.

**FINANCIAL INSTITUTIONS**
Litigation and bankruptcy checks for companies and debtors.

**E-DISCOVERY AND LEGAL VENDORS**
Sync your system to PACER to automate legal marketing.